Coordination Chemistry Reviews 253 (2009) 2912–2919

Contents lists available at ScienceDirect

Coordination Chemistry Reviews

journal homepage: www.elsevier.com/locate/ccr

Atomic detail observation of adsorbed molecules and metal clusters on carbon nanotube electron emitters

Yahachi Satio*

Department of Quantum Engineering, Nagoya University, Furo-cho, Chikusa-ku, Nagoya 464-8603, Japan

ARTICLE INFO

Article history:
Received 2 April 2009
Accepted 31 July 2009
Available online 7 August 2009

Keywords:
Adsorption
Field emission microscopy
Carbon nanotube
Gaseous molecule
Aluminum

ABSTRACT

Molecular images and dynamics of adsorbates on carbon nanotube (CNT) electron emitters revealed so far by field emission microscopy (FEM) are reviewed after a brief account of the field emission phenomena and the merit of CNTs as the field emitter. The species adsorbed on CNTs are inorganic and organic common gaseous molecules (H_2, N_2, O_2, CO, CO_2, CH_4) and aluminum (Al) clusters. In the case of N_2 and CO_2 molecules, dumbbell-shaped images, reflecting their molecular shapes, have been observed. For the case of Al deposition on CNTs, FEM images revealing atomic detail of an Al cluster with the cubo-octahedron structure were observed. Discussion on the spatial resolution in FEM for CNTs suggests the probable observation of some atomic structures with a resolution of the order of 0.3 nm.

1. Introduction

Field emission of electrons from a single carbon nanotube (CNT) and a film of CNTs was first reported, respectively, by Rinzler et al. [1] and by de Heer et al. in 1995 [2]. Saito et al. reported a field emission microscopy (FEM) study of CNTs in 1997 [3,4]. Since then, cathode-ray tube (CRT)-type lighting elements with CNT field emitters [5], CNT-based field emission display (FED) [6–11] and back-light units [12] have been experimentally manufactured and their high performance is demonstrated. Among various applications of CNTs proposed so far, field emission electron sources would be the most promising industrially and are nearly within the reach of practical use.

FEM images obtained from a capped multiwall carbon nanotube (MWCNT) with clean surfaces exhibit fine structures originating from carbon pentagons at its tip and interference fringe of emitted electron waves [13]. Pentagonal rings with a small dark spot in their center are imaged on a fluorescence screen, but the five carbon atoms forming a pentagon, the nearest neighbor distance of which is 0.144 nm, are not resolved.

The pentagonal ring patterns characteristic of capped MWCNTs are observed when the surface of a CNT cap is clean. When a gas molecule adsorbs onto a clean MWCNT cap, the molecule appears as a bright spot in the FEM image and a sudden increase in emission current is observed [14]. FEM experiments give insight of the behavior of gas molecule adsorbed onto a clean pentagon and their effect on the electron emission from CNT emitters.

In this article, molecular images and dynamics of adsorbates on CNT electron emitters revealed so far by FEM are reviewed after a brief account of the field emission phenomena and the merit of CNTs as the field emitter. The species adsorbed on CNTs are inorganic and organic common gaseous molecules (H_2, N_2, O_2, CO, CO_2, CH_4) and aluminum clusters. In the case of N_2 and CO_2 molecules, dumbbell-shaped images, reflecting their molecular shapes, are recently observed by FEM [15,16]. For metal species, on the other hand, various unusual FEM images from metal tips and whiskers were reported in the 1950s [17], and the controversy as to whether FEM can reach atomic resolution or not reached its peak. However, the advent of impressive atomic resolution images by helium field ion microscopy (FIM) by Müller and Badabur [18] in 1956 faded out the controversy, and the question has remained pending ever since. In 1956, Rose [19] proposed a resolution equation for FEM, and suggested that atomic resolution in FEM is possible if the tip radius is small enough. Finally, the possibility of atomic imaging of protruding structures on CNT tips by FEM is discussed.

2. Field emission and Fowler–Nordheim model

When a high electric field on the order of 10^7 V/cm is applied to a solid surface with a negative electrical potential, electrons inside the solid are emitted into vacuum by the quantum mechanical tunneling effect. This phenomenon is called field emission of electrons. Such an extremely high field can be obtained on a surface in close proximity (several to tens of nanometer) to a counter electrode or on a sharp tip of a very thin needle-like CNTs.

* Tel.: +81 52 789 4459; fax: +81 52 789 3703.
E-mail address: ysaito@nagoya-u.jp.

0010-8545/$ – see front matter © 2009 Elsevier B.V. All rights reserved.
doi:10.1016/j.ccr.2009.07.027

The current density J [A/m^2] of electrons emitted from a flat unit surface by field emission, which is known as Fowler–Nordheim equation [20,21], is expressed as

$$J = \frac{1.54 \times 10^{-6} F^2}{\phi} \exp\left(-\frac{6.8 \times 10^9 \phi^{3/2}}{F}\right) \quad (1)$$

where F is the electric field strength in V/m, ϕ the work function of the surface in eV. This equation is correct only for an abrupt potential drop at the metal surface. When the effect of an image charge is taken into account, the two constants in Eq. (1) are modified depending on F and ϕ. It should also be noted that the Fowler–Nordheim equation is derived under the following assumptions: electrons inside the surface are treated as free electron gas, the temperature is 0 K, and the tunneling is elastic and occurs from a flat surface.

Various modifications of the Fowler–Nordheim model for semiconductors and protruding surfaces (non-flat surfaces) have been developed [22,23]. Actually, field emission (FE) current is very sensitive to not only geometrical structure of the emitter tip but also the work function and adsorbates.

3. Advantages of carbon nanotubes as field emitters

CNTs have the properties favorable as field emitters: (1) needle-like shape with a sharp tip, (2) high chemical stability, (3) high mechanical strength, (4) low carbon atom mobility, and (5) high electrical and thermal conductivity. The needle-like morphology with an extremely small radius of curvature at the tip is the most prominent advantage of CNTs as electron emitter. When an electric field is applied to a conductor with a sharp tip, it concentrates at the sharp point. The field strength at the tip surface is inversely proportional to the radius of curvature r of the tip [24]. The surface of a CNT is inert and stable against residual gas molecules in a vacuum vessel because of chemical stability of graphite material which constitute CNTs. High mechanical strength (tensile strength ~100 GPa [25]) of CNT emitters enables them to endure the high stress caused by electrostatic forces (Maxwell tension). Together with this robustness, low mobility of carbon atoms in CNTs make them keep their original shape (slender and sharp tip) even under high electric field. Finally, since CNTs, especially MWNTs formed by arc discharge, have high electrical and thermal conductivity, CNTs can transport and emit electrons of high current density (ca. 10^7 A/cm^2) through their tubular walls into vacuum [26].

4. Field emission microscopy (FEM) of carbon nanotubes

4.1. FEM measurement

Field emission microscopy (FEM) enables us to image the spatial distribution of the emitted electron current of a single emitter, by using a phosphor screen as an anode. The emitter is usually mounted on a heating loop (e.g., hairpin-shaped tungsten wire with diameter of 0.15 mm) for cleaning the tip apex by desorbing absorbed molecules. The emission of a metallic tip should be homogeneous (at least over the tip apex if the work function is constant), while emission from localized states or from adsorbates produces well-defined patterns. FEM provides us with important information on the emission mechanism and surface phenomena on a CNT [27,28].

For FEM study, it would be ideal to use a single, isolated CNT fixed at the apex of a metal needle. Such emitters are tried to be prepared by using micromanipulators in a scanning electron microscope [29], but the emitters thus prepared are usually covered with contaminants (hydrocarbon deposit) during the SEM observation. Electrophoresis is an alternative method to attach a thin bundle of CNTs at the tip of a metal needle [30], though the control of the number of CNTs in an attached bundle is difficult. The simple and easy method is to glue a bulk bundle of as-grown CNTs to the tip of a heating loop by using a conductive paste [31]. The last method keeps tips of CNTs clean, but the enormous number of CNTs is protruding out at the end of the bundle.

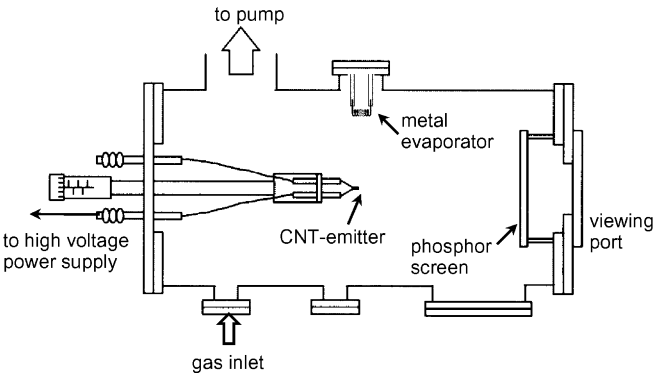

Fig. 1. Schematic of a FEM apparatus.

A schematic of a FEM apparatus is shown in Fig. 1. The emitter tip of CNTs is placed at about 30 mm distance from a phosphor screen, on which field emission patterns can be observed. The base pressure of the FEM vacuum chamber is 10^{-7} to 10^{-8} Pa [13,14,31]. The negative voltage of 0.6 kV to 1.6 kV was applied to the emitter relative to the screen.

4.2. Multiwall carbon nanotubes with clean surfaces

Multiwall carbon nanotubes (MWCNTs) produced by arc discharge technique [32,33] are highly graphitized (i.e., composed of well developed graphene layers) and thus have high structural perfection. The ends of arc-grown MWCNTs are capped by graphite layers with polyhedral shapes as shown in Fig. 2. In order to give a positive curvature to a hexagon sheet, pentagons (five-membered carbon rings) have to be introduced to the sheet; six pentagons are required to have a curvature of 2π steradian (i.e., a hemispherical cap) [34]. The portion where a pentagon is located extrudes like a vertex of a polyhedron, while the other flat regions are made of hexagons.

Typical FEM images of MWCNT emitters with clean surfaces are shown in Fig. 3. Clean CNT tips are acquired by heating at about 1000 °C for a few minutes in ultrahigh vacuum chamber (e.g., 10^{-8} Pa) by which adsorbates on CNT surfaces are desorbed [14]. Six pentagonal rings arranged in fivefold (Fig. 3(a)) and sixfold symmetry (Fig. 3(b)) can be observed. Each pentagonal region contained a small dark spot at its center. It should also be noted that interference fringes are observed between the neighboring pentagons. Structural models of CNT tips that would give the FEM patterns in Fig. 3(a) and (b) are shown in Fig. 4(a) and (b), respectively.

Since the pentagons are locally extruding like vertices, the electric field around them would be stronger than that on other flat regions. In addition, it is theoretically indicated that the pentagon site has a higher density of states (DOS) near the Fermi level E_F than the normal hexagon site [35]. Therefore, the electron tunneling through the pentagons are expected to occur dominantly.

Such patterns consisting of arranged pentagons changes when gas molecules adsorb on the CNT cap. An adsorbed molecule is usually imaged as a bright spot in the FEM picture, giving rise to an abrupt increase in the emission current [14]. Similar stepwise fluctuations of emission current are also frequently observed in other FE electron sources [36,37]. The origin of the stepwise changes is the adsorption and desorption of molecules on the surface of the

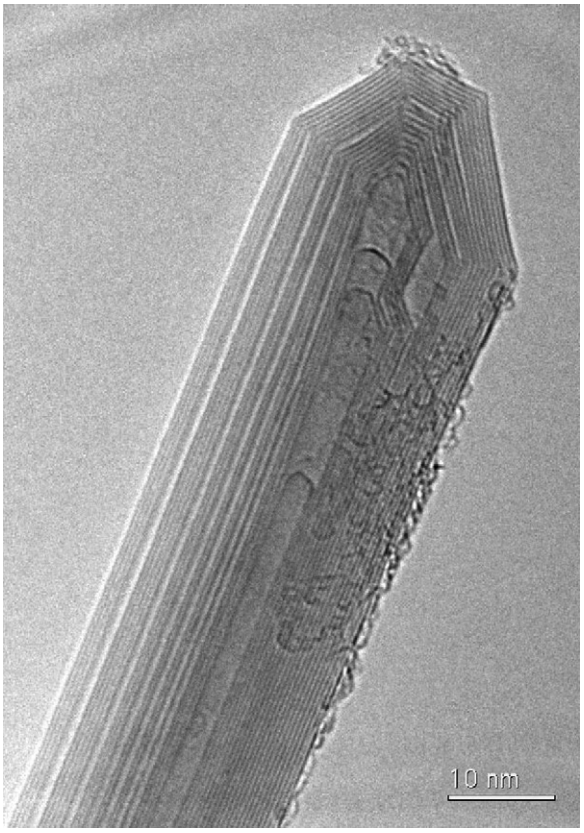

Fig. 2. TEM picture of an MWNT produced by arc-discharge method.

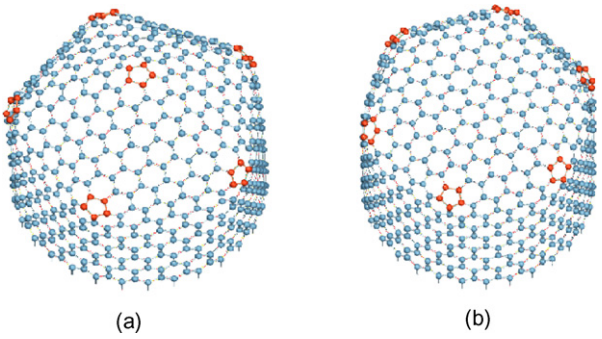

Fig. 4. Structural models of CNT tips that would give the FEM patterns in (a) and (b).

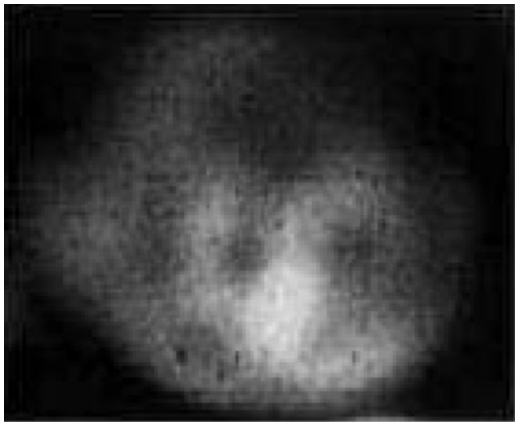

Fig. 5. FEM pattern of single-wall CNTs (SWCNTs). After Dean and Chalamala [38].

emitter. Though most of adsorbed molecules in the FEM images appear simple, bright spots (structure-less), but some molecules exhibit characteristic shapes reflecting the molecular structure as described in the next section.

Emission patterns from open-ended MWCNTs, which were prepared by oxidation processes, showed bright "doughnut-like" annular rings, reflecting the geometry of the CNT tip [4].

4.3. Single-wall carbon nanotubes

FEM of MWCNTs with closed-caps show clear pentagon images, but that of single-wall CNTs (SWCNTs), as shown in Fig. 5, do not show pentagonal rings but dim (blurred) patterns which resemble scanning tunneling microscope (STM) images of C_{60} fullerenes [38]. Experimental study using CNTs with different apex radii [39] suggested that the difference in the FEM images originate from the difference in the radius of curvature of CNT tips; the "pentagon" patterns are observed for CNTs with apex radii larger than ca. 2 nm while the "dim" patterns for those with smaller apex radii.

According to the argument on the spatial resolution of FEM [19,40], resolutions of 0.2 nm and 0.35 nm are possible for emitters with tip radius 1 nm and 4 nm, respectively. However, it is not enough to resolve individual atoms on the CNT caps. Since the pentagon–pentagon separation s_{p-p} on a CNT cap is roughly the same as the radius of tip curvature [39], the s_{p-p} which differentiates the patterns is approximately 2 nm.

Enhanced FE from adsorbates has been observed in the case of SWCNTs as well. Dean et al. showed three distinct behavior states in FE from SWCNTs at temperatures ranging from 300 K to 1800 K [41]. At room temperature, emission occurred through adsorbate states, which they considered to be correlated to the presence of

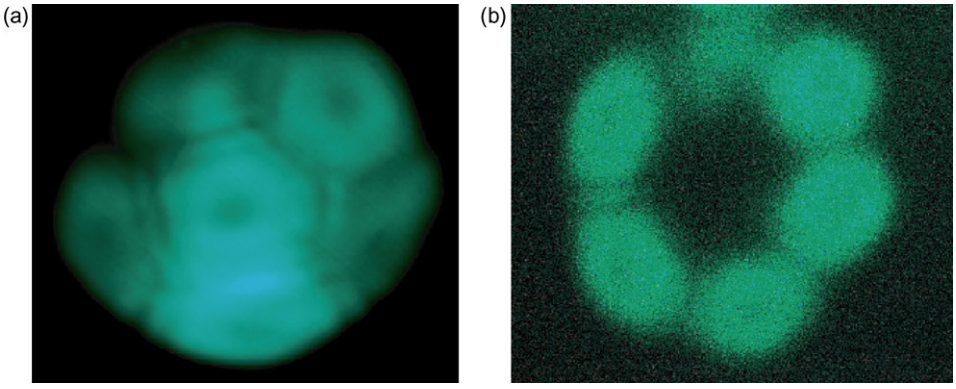

Fig. 3. Typical FEM images of MWNT emitters with clean surfaces. Six pentagonal rings are arranged in fivefold (a) and sixfold symmetry (b).

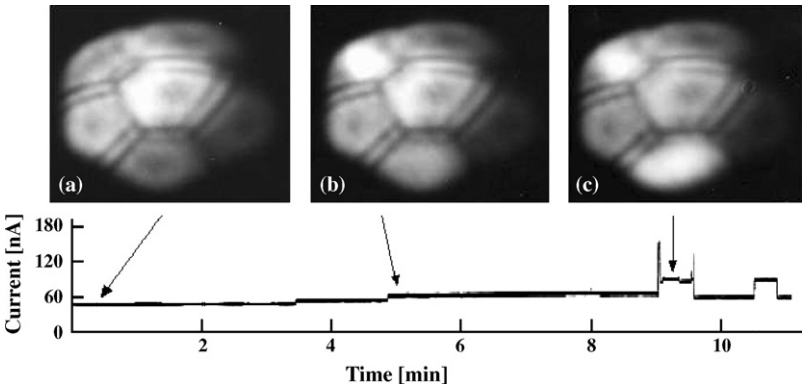

Fig. 6. A time-sequential series of FEM patterns from an MWCNT exposed to hydrogen gas at pressure of 1×10^{-8} Torr and the corresponding changes in the emission current [42].

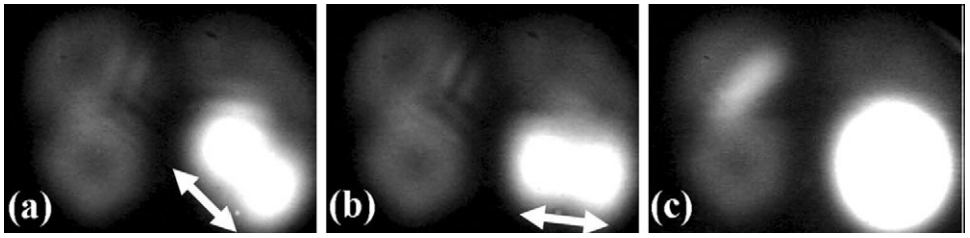

Fig. 7. Two types of FEM pattern of a nitrogen molecule [15]. (a and b) "Cocoon"-shaped images with different orientations, and (c) bright circular spot.

water, since partial pressure of water is dominant in an unbaked vacuum chamber. These states were removed above 900 K. After adsorbate removal, the apparently clean CNT state showed a lower emission current and substantially reduced emission noise. Upon transition to the low current regime, the lobed patterns due to adsorbed states disappeared, and dimmer FEM patterns with finer structures, which were considered to originate from clean SWCNT caps, were observed.

5. Field emission from adsorbates on an MWCNT

5.1. Molecules

5.1.1. Hydrogen

Fig. 6 shows a time-sequential series of FEM patterns from an MWCNT exposed to hydrogen gas at pressure of 1.3×10^{-6} Pa and the corresponding changes in the emission current [42]. The pentagon pattern characteristic of a clean MWCNT cap just after flashing (Fig. 6(a)) changed to FEM patterns in which one or two small bright spots appeared on the pentagon pattern as shown in Figs. 6(b) and (c), and the slight increase in the emission current occurred concurrently with the appearance of a bright spot. The number and the position of bright spots changed randomly, indicating that adsorption and desorption of hydrogen molecules occurred frequently on the CNT cap, preferentially on pentagon sites where electric field concentrates. After the FE measurement for 11 min with the emission current of 50–100 nA, the hydrogen gas was evacuated and the CNT emitter was subjected to flashing. By this cleaning process, the emission pattern recovered to the original clean pattern, suggesting that hydrogen molecules are inert for the surfaces of MWCNTs under this FE condition.

5.1.2. Nitrogen

Fig. 7 shows two types of FEM image of an adsorbate in an atmosphere of nitrogen gas of 8×10^{-7} Pa [15]. A bright spot, which appears on a pentagon site, changes its brightness and shape. The image is "cocoon"-shaped (Figs. 7(a) and (b)) when the current is small, while the image is a bright circular spot (Fig. 7(c)) when the emission current is large. A model explaining two different adsorption states of a single nitrogen molecule is shown in Fig. 8. If the molecular axis of nitrogen is parallel to the substrate pentagon, as illustrated in Fig. 8(a), the bright spot corresponding to the nitrogen will exhibit a cocoon shape reflecting a shape of the molecule (interatomic distance of N_2: 0.1094 nm). When the molecular axis is perpendicular to the substrate (Fig. 8(b)), on the other hand, the emission pattern should be a circular bright spot. In the latter configuration, the extended protrusion enhances the field concentration and thus brings about the enhanced emission current, i.e., brighter spot. The effect of the electric field on the adsorbed molecules is considered to become visible in this configuration; the perpendicular configuration of the molecule is expected to gain larger adsorption energy than the parallel configuration because

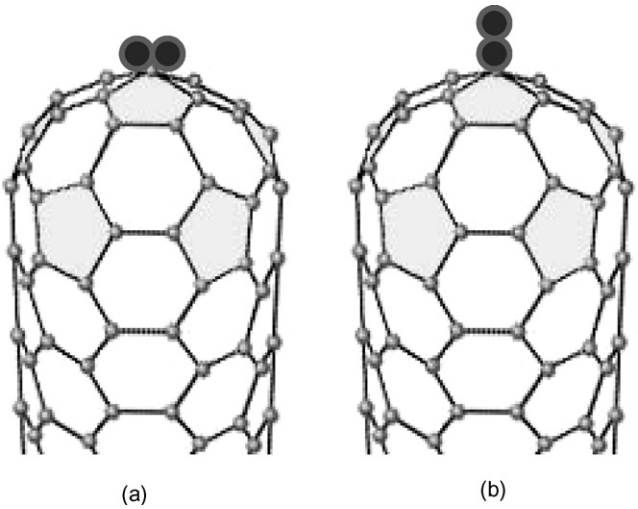

Fig. 8. A model explaining two different adsorption states of a single nitrogen molecule. The molecular axis is (a) parallel to and (b) perpendicular to the substrate.

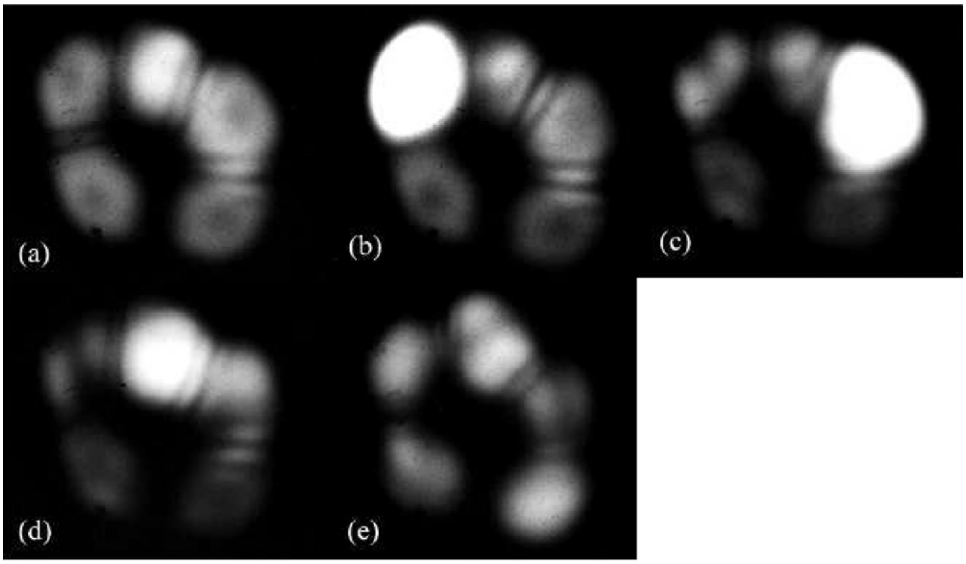

Fig. 9. FEM images of an MWCNT exposed to oxygen gas [42].

the larger polarization force is induced in the perpendicular configuration.

5.1.3. Oxygen

FEM images of an MWCNT exposed to oxygen gas are shown in Fig. 9 [42]. The FEM image before the exposure to oxygen (Fig. 9(a)) changed to those (Fig. 9(b)–(d)) after the introduction of oxygen up to 1×10^{-8} Torr. Adsorption and desorption occurred frequently at the pentagon sites, which is similar to the case of hydrogen or nitrogen, but the pentagonal rings were not recovered after the disappearance of bright spots. This suggests that pentagons were damaged during electron emission in the oxygen atmosphere. After the FE experiment for 10 min, the MWCNT emitter was heated (1300 K for 1 min) again in an ultrahigh vacuum in order to desorb oxygen molecules. Fig. 9(e) shows the FEM pattern obtained after the heat treatment. All the pentagons are damaged, and the original pattern shown in Fig. 9(a) is no longer reproduced, exhibiting very high reactivity of oxygen against the CNT surfaces.

5.1.4. Carbon monoxide

When carbon monoxide was introduced into the FEM chamber up to the pressure of 1.3×10^{-6} Pa, large bright spots corresponding to adsorption of molecules appeared like oxygen adsorption. Even though the emitter was tried to be cleaned by heating in an ultrahigh vacuum after the electron emission for 600 s, the bright spot on the top pentagon did not disappeared, and the clean pentagon's pattern was not recovered. This suggests that a carbon monoxide molecule was strongly bonding to the pentagon, or it damaged to the pentagon by the thermal desorption.

5.1.5. Carbon dioxide

FEM images of a single CO_2 adsorbed on an MWCNT also exhibited a cocoon-shaped bright spot as in Fig. 10 [16]. Even though a CO_2 molecule is triatomic, it looks like diatomic similar to a nitrogen admolecule shown in the previous section. The cause of exhibiting the cocoon shape is probably the electric charge distribution within a CO_2 molecule, in which electron cloud leans toward the outer oxygen atoms from the centered carbon atom.

Though the CO_2 admolecule in Fig. 10 moved randomly and discretely on the substrate pentagon with time interval of order of 100 ms, the orientation of the long axis of the admolecule is found to be divided statistically equally into five orientations, suggesting the presence of five equivalent stable adsorption sites (orientations) for a CO_2 on the pentagon. The angles between the molecular axes of the adjacent orientations are in average 36° with a slight deviation of only a few degrees, being in good agreement with the angle expected for the symmetry of the pentagon. The length of diago-

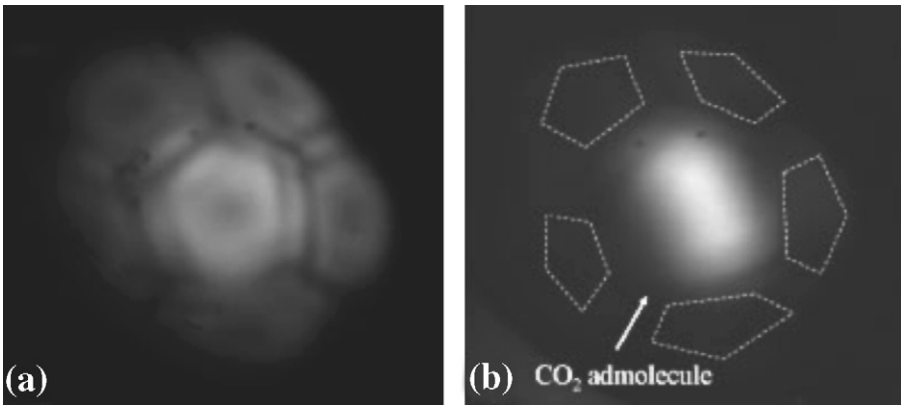

Fig. 10. FEM images of (a) a clean MWCNT tip and (b) a single CO_2 adsorbed on it [16]. A CO_2 molecule exhibits a cocoon shape, whose orientation changes randomly among the five discrete directions.

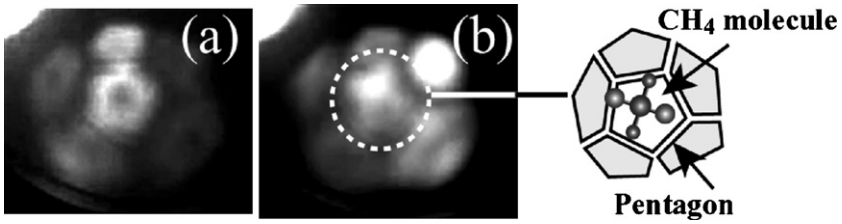

Fig. 11. FEM images of (a) before and (b) after adsorption of a methane molecule on a pentagon at the MWCNT tip. A cross-shaped image, reminiscent of a CH_4 molecule looked along the twofold rotational symmetry axis, is observed in (b).

nal lines for the carbon pentagon with a side length of 0.142 nm, i.e., C–C bond length of graphite, is 0.230 nm. This length is in good agreement with the interatomic distance of both side oxygen atoms in CO_2 molecule, i.e., 0.233 nm. Details of the adsorption sites and the motion of a CO_2 on the carbon pentagon are discussed in Ref. [16], in which the rotation angle of 72°, instead of 36°, is asserted from an analysis of motion in the video file from frame to frame (time interval of 1/30 s), and the rotation of the molecules around the centered carbon atom is suggested.

5.1.6. Methane

Investigation of the effect of electric field on methane adsorption has revealed that methane adsorption occurs only when the emitter was applied negative electric voltage (i.e., being biased to emit electrons) whereas no methane adsorption was observed when positive voltage is applied or no voltage applied in an atmosphere of 1.0×10^{-7} Pa methane gas [43].

FEM images of adsorbed methane molecules are usually simple bright spots like inorganic molecules such as H_2, O_2 and CO mentioned above. Occasionally, however, a cross-shaped image is observed as shown in Fig. 11. Since a CH_4 molecule has the tetrahedral structure, it looks like a "cross" shape when its twofold symmetry axis is normal to the substrate. The size of the cross image is roughly measured to be 0.23 nm on the basis of the size of a pentagon, which was observed under the admolecule. Compared with the size of CH_4 (0.21 nm, the distance between two hydrogen atoms of a methane molecule), the FEM gives a little larger image than the real size. This is presumably due to an enhanced magnification of a small protrusion on a round emitter surface [19]. From the shape and the size of the image, we assume that the pattern corresponds to a single molecule of methane.

5.1.7. Comparison with related theoretical studies

Theoretical studies, which can be compared with FEM images presented in this article or explain them, are not available now, while the variations of emission current due to adsorption of some molecules have been discussed theoretically. According to Wadhawan et al. [44], adsorption of commonly electronegative gases, for example, O_2 and NH_3, can decrease the current, and inert gases such as He and Ar barely affect the FE current and its stability. This theoretical prediction contradicts the experimental observation at least for the O_2 adsorption. Park et al. [45] ascribed the experimentally observed emission increase by oxygen adsorption to the local enhancement of electric field and a creation of new electronic states.

Li and Wang [46] predicted that the adsorption of CO and CH_4 decrease the emission current because of the increase in work function. Sheng et al. [47], on the other hand, predicted that CO and CO_2 decrease the current, but CH_4 increases it. Contradictions between various theoretical studies themselves are found. Experimentally, all kinds of molecules brought about emission enhancement upon their adsorption on a CNT.

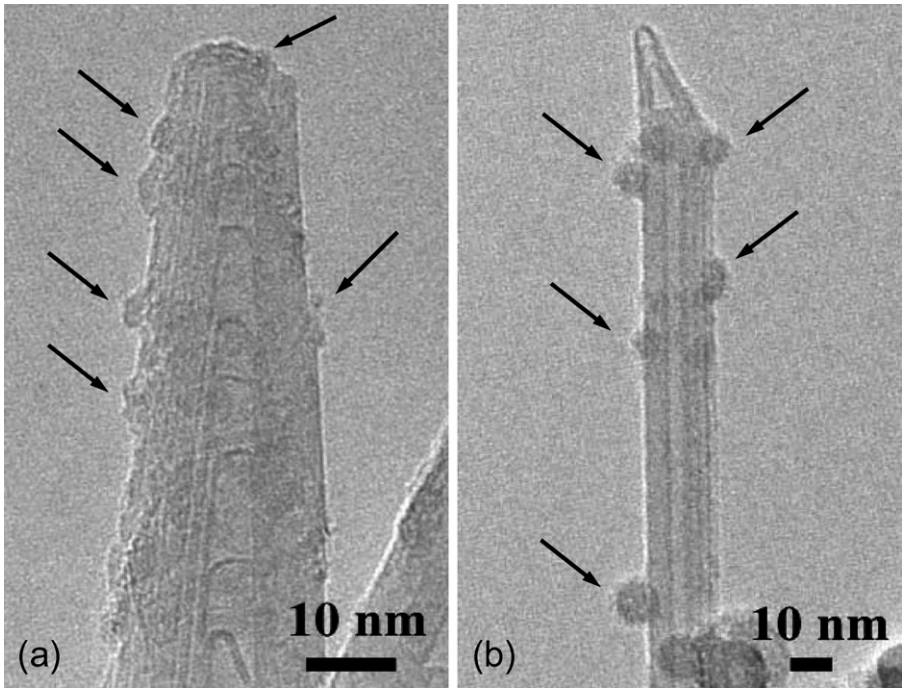

Fig. 12. TEM images of Al-deposited MWCNTs (a) before and (b) after field emission. Mean thickness of deposited Al is 2.5 nm. Arrows indicate Al clusters. Different MWCNTs are shown in (a) and (b).

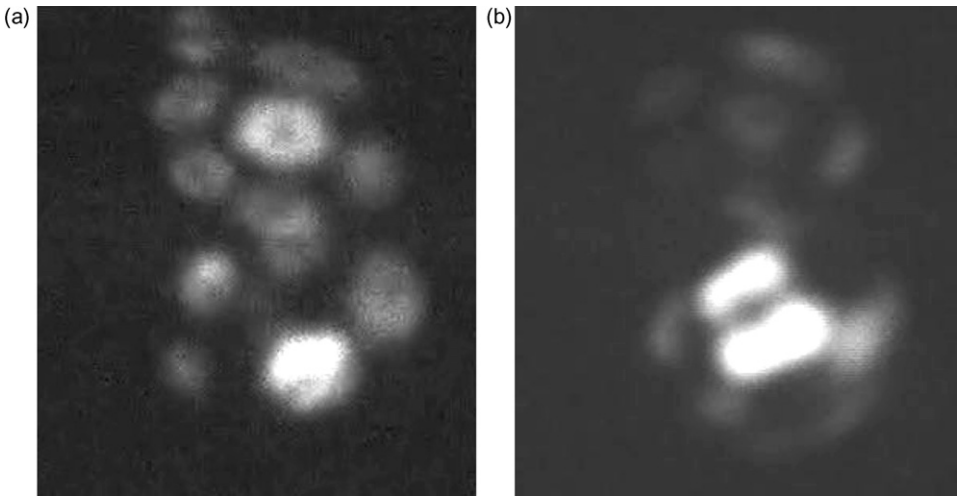

Fig. 13. FEM images of (a) clean MWNT caps and (b) an Al cluster on an MWNT tip.

5.2. Aluminum clusters

Fig. 12(a) shows a transmission electron microscope (TEM) picture of Al with mean thickness of 2.5 nm deposited on MWNTs before the FE experiment. The deposited Al formed a discontinuous film consisting of isolated islands with diameter of a few nm. After the FE experiment, diameter of Al clusters increased to about 10 nm as revealed by Fig. 12(b).

During the study on the effect of Al deposition by FEM, intriguing FEM images suggestive of an Al cluster with atomic resolution were observed [48]. Fig. 13(a) and (b) shows FEM images of an MWCNT emitter before and after Al deposition, respectively. A spotty pattern with a high symmetry (fourfold symmetry in this case) appeared on the pentagon patterns characteristic of clean caps of MWCNTs (two MWNTs are visible in this image) after the Al deposition, as shown in Fig. 13(b). The contrast of the spotty pattern is reminiscent of the structure of an atom cluster with a shape of cubo-octahedron, which is a crystal form characteristic of face-centered cubic metals [49]. A model of the structure consisting of 38 Al atoms is illustrated in Fig. 14. The fourfold symmetry of the Al image suggests that the Al cluster is oriented with its [1 0 0] direction normal to the nanotube surface. Four bright spots observed in the central part of the Al image correspond to four corners of the top (1 0 0) surface. Four dark regions surrounding the central (1 0 0) face correspond to (1 1 1) faces, which are outlined by bright edges and corners.

The distance between neighboring atoms along the edge of the (1 0 0) surface is 0.286 nm when the lattice constant of the cluster is the same with that of bulk Al. Using the size of the carbon pentagon (approximately 0.25 nm in diameter) as a measure of magnification of FEM images, under an assumption that the pentagon image originates from five carbon atoms comprising a pentagon, the distance between the bright spots at the corners of the (1 0 0) face is estimated to be in a range from 0.28 nm to 0.31 nm, being in good agreement with the nearest neighbor distance on the Al (1 0 0) surface. In this case, the magnification enhancement due to a small protrusion on a round tip seems not to be so large.

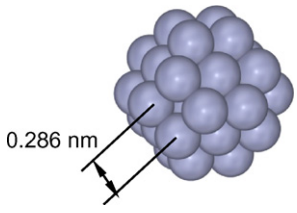

Fig. 14. Cubo-octahedron of an Al_{38} cluster.

Metal clusters or nanoparticles often exhibit atomic structures different from crystal structures in bulk, e.g., icosahedral or multiply twinned structures for elements which form fcc structures in bulk. For Al, however, icosahedral structures have never been observed ever for small particles by electron microscopy [49]. Theoretical calculations also suggest that the structural transition from the fcc to the icosahedron structures lies in a range of size between 13- and 55-atom clusters [50]. The present Al cluster falls in this transition range in size. Thus, it is highly probable that the Al cluster exhibits the same structure with the bulk.

The polyhedral Al cluster (Fig. 13(b)), exhibiting rotation and migration, disappeared in several seconds from the field of view after its appearance, and finally the original clean cap was recovered. The migration and diffusion of Al clusters on MWCNTs are responsible for the increased diameter of Al clusters observed by TEM after the FE experiment as shown in Fig. 12(b).

6. Resolution in FEM and possible observation of atomic detail

In 1956, Rose [19] gave the equation of FEM resolution δ, which consists of the two principal components, namely, the momentum uncertainty and the effect of the transverse velocities of the electrons near the top of Fermi level in the emitter:

$$\delta = \left(\frac{2\hbar\tau}{mM}\right)^{1/2}\left(1+\frac{2m\tau {v_0}^2}{\hbar M}\right)^{1/2} \quad (2)$$

where M is magnification, τ is the time-of-flight of an electron from emission tip to screen, v_0 is the average transverse velocity, $\hbar$ is Planck's constant/2π, and m is the electron mass. When M/τ is large enough to assume $2m\tau v_0^2/\hbar M \ll 1$, the term containing v_0 become negligible and the resolution is limited by the uncertainty principle. Under such a condition, say $M/\tau \approx 2.5 \times 10^{15}$, he suggested that small protrusions on the surface of the tip can provide resolution of the order of 0.3 nm so that some of their atomic detail should be observable. M is always reduced by a factor β from that expected for a spherically symmetric geometry where the tip and screen are assumed to be concentric spheres of radii R and z, i.e.,

$$M = \frac{z}{\beta R} \quad (3)$$

Using the approximation $\beta \approx 1.9$, $\tau \approx z(2\,\mathrm{eV/m})^{-1/2}$ and $v_0 \approx 2 \times 10^5\,\mathrm{m/s}\,(= 0.11\,\mathrm{eV})$, the following practical form of resolution equation [19,40] is obtained:

$$\delta = 0.860\left(\frac{R}{\sqrt{V}}\right)^{1/2}\left(1 + \frac{2.22R}{\sqrt{V}}\right)^{1/2} \quad (4)$$

where δ is in nm, R is the tip radius in nm, and V is the applied potential in volts between the tip and screen.

From Eq. (4), we see that atomic resolution is attainable for $R/\sqrt{V} < 1$. In the experiment using an MWCNT as an emitter, R and V are about 5 nm and the applied voltage of 1.5 kV, respectively. These parameters give a resolution of the order of 0.3 nm, indicating that some of atomic detail is observable in the present experimental condition.

7. Conclusions

The phenomena of electron field emission from CNTs and their applicability to vacuum electronic devices such as field emission displays and lamps have been intensively studied since the first reports illustrating intriguing and excellent field emission properties of CNTs [1,2]. CNTs possess unique structural and physicochemical properties distinctive from traditional metal emitters (e.g., tungsten and molybdenum); extremely small tip radius (1 to 10 nm), well defined, stable surface structures (composed of carbon hexagons and pentagons) made of strong C–C bonds, no oxide formation and no surface diffusion of carbon atoms. This article focuses on the fundamental properties of CNT field emitters, and reviews recent FEM studies suggesting near-atomic resolution images of adsorbed molecules and metal clusters. The high resolution is probably due to the small tip radius of these CNT emitters as suggested by Rose's estimation of resolution [19] though it is rather old. The appearance of pentagons in FEM images, as a measure of magnification of the images, is another merit of CNT emitters. Adsorbed molecules shown in this review are small common molecules such as N_2 and CO_2. When metal (W or Mo) needles were employed as FEM emitter, such molecular images reflecting their structures were never observed because of presumable reactions between an admolecule and the metal surface. The chemical inertness of CNT surfaces is responsible for the stable observation of these small molecules.

In the 1950s, there was controversy as to whether objects of atomic dimensions can be resolved by FEM. The most interesting and yet controversial FEM patterns are quadruplet or doublet patterns originating from organic dye molecules such as phthalocyanine or flavanthrene reported first by Müller [51]. The advent of CNTs as field emitters will revive the discussion on FEM resolution and open a new focus on the FEM technique for direct observation of adatoms and admolecules. For developing the FEM technique, a realistic theory applicable to CNT emitters is seriously required since the simple F–N theory is inadequate for the more sophisticated analysis of FEM observations.

References

[1] A.G. Rinzler, J.H. Hafner, P. Nikolaev, L. Lou, S.G. Kim, D. Tománek, P. Nordlander, D.T. Colbert, R.E. Smalley, Science 269 (1995) 1550.
[2] W.A. de Heer, A. Châtelain, D. Ugarte, Science 270 (1995) 1179.
[3] Y. Saito, K. Hamaguchi, T. Nishino, K. Hata, K. Tohji, A. Kasuya, Y. Nishina, Jpn. J. Appl. Phys. 36 (1997), L1340.
[4] Y. Saito, K. Hamaguchi, K. Hata, K. Uchida, Y. Tasaka, F. Ikazaki, M. Yumura, A. Kasuya, Y. Nishina, Nature 389 (1997) 554.
[5] Y. Saito, S. Uemura, K. Hamaguchi, Jpn. J. Appl. Phys. 37 (1998), L346.
[6] S. Uemura, T. Nagasako, J. Yotani, T. Shimojo, Y. Saito, Society for Information Display, 1998 Int. Sym., Digest of Technical Papers, 1998, p. 1052.
[7] W.B. Choi, D.S. Chung, J.H. Kang, H.Y. Kim, Y.W. Jin, I.T. Han, Y.H. Lee, J.E. Jun, N.S. Lee, G.S. Park, J.M. Kim, Appl. Phys. Lett. 75 (1999) 3129.
[8] J. Yotani, S. Uemura, T. Nagasako, H. Kurachi, T. Nakao, M. Ito, A. Sakurai, H. Shimoda, T. Ezaki, K. Fukuda, Y. Saito, Society for Information Display, 2008 Int. Sym., Digest of Technical Papers, 2008, p. 151.
[9] Y.C. Choi, K.S. Jeong, I.T. Han, H.J. Kim, Y.W. Jin, J.M. Kim, B.G. Lee, J.H. Park, D.H. Choe, Appl. Phys. Lett. 88 (2006) 263504.
[10] K.A. Dean, H. Li, B.F. Coll, E. Howard, S.V. Johnson, M.R. Johnson, D.C. Jordan, L. Marshbanks, L.H. Tisinger, M. Hupp, S. Wieck, E. Weisbrod, S. Smith, S.R. Young, J. Barker, D. Weston, W.J. Dauksher, Y. Wei, J.E. Jaskie, Society for Information Display, 2006 Int. Sym., Digest of Technical Papers, 2006, p. 1845.
[11] T. Tonegawa, M. Taniguchi, S. Itoh, K. Nawamaki, Y. Marushima, Y. Kubo, Y. Fujimura, T. Yamaura, Proc. Int. Display Workshop, 2005, p. 1659.
[12] Y.C. Kim, H.S. Kang, E. Cho, D.Y. Kim, D.S. Chung, I.H. Kim, In.T. Han, J.M. Kim, Nanotechnology 20 (2009), 095204.
[13] Y. Saito, K. Hata, T. Murata, Jpn. J. Appl. Phys. 39 (2000), L271.
[14] K. Hata, A. Takakura, Y. Saito, Surf. Sci. 490 (2001) 296.
[15] S. Waki, K. Hata, H. Sato, Y. Saito, J. Vac. Sci. Technol. B 25 (2007) 517.
[16] Y. Kishimoto, K. Hata, Surf. Interface Anal. 40 (2008) 1669.
[17] A.J. Melmed, R. Gomer, J. Chem. Phys. 30 (1959) 586.
[18] E.W. Müller, K. Badabur, Phys. Rev. 102 (1956) 624.
[19] D.R. Rose, J. Appl. Phys. 27 (1956) 215.
[20] L.W. Nordheim, Proc. R. Soc. Lond., Ser. A 121 (1928) 626.
[21] E.L. Murphy, R.H. Good, Phys. Rev. 102 (1956) 1464.
[22] A. Modinos, Field, Thermionic and Secondary Electron Emission Spectroscopy, Plenum, New York, 1984.
[23] J. He, P.H. Cutler, N.M. Miskovsky, T.E. Feuchtwang, T.E. Sullivan, M. Chung, Surf. Sci. 241 (1991) 348.
[24] R. Gomer, Field Emission and Field Ionization, Harvard University Press, Cambridge, MA, 1961.
[25] B.G. Demczyk, Y.M. Wang, J. Cumings, M. Hetman, W. Han, A. Zettl, R.O. Ritchie, Mater. Sci. Eng. A 334 (2002) 173.
[26] B.Q. Wei, R. Vajtai, P.M. Ajayan, Appl. Phys. Lett. 79 (2001) 1172.
[27] J.W. Gadzuk, E.W. Plummer, Rev. Mod. Phys. 45 (1973) 487.
[28] A.J. Melmed, E. Müller, J. Chem. Phys. 29 (1958) 1037.
[29] Y. Nakayama, H. Nishijima, S. Akita, K.I. Hohmura, S.H. Yosimura, K. Takeyasu, J. Vac. Sci. Technol. B 18 (2000) 611.
[30] Y. Saito, K. Seko, J. Kinoshita, Diam. Relat. Mater. 14 (2005) 1843.
[31] Y. Saito, K. Hamaguchi, K. Hata, K. Tohji, A. Kasuya, Y. Nishina, K. Uchida, Y. Tasaka, F. Ikazaki, M. Yumura, Ultramicroscopy 73 (1998) 1.
[32] S. Iijima, Nature 354 (1991) 56.
[33] Y. Saito, T. Yoshikawa, M. Inagaki, M. Tomita, T. Hayashi, Chem. Phys. Lett. 204 (1993) 277.
[34] M. Endo, K. Takauchi, K. Kobori, K. Takahashi, H.W. Kroto, A. Sarkar, Carbon 33 (1995) 873.
[35] R. Tamura, M. Tsukada, Phys. Rev. B 52 (1995) 6015.
[36] S. Yamamoto, S. Hosoki, S. Fukuhara, M. Futamoto, Surf. Sci. 86 (1979) 734.
[37] Y. Ishizawa, T. Aizawa, S. Otani, Appl. Surf. Sci. 67 (1993) 36.
[38] K.A. Dean, B.R. Chalamala, J. Appl. Phys. 85 (1999) 3832.
[39] Y. Saito, Y. Tsujimoto, A. Koshio, F. Kokai, Appl. Phys. Lett. 90 (2007) 213108.
[40] I. Brodie, Surf. Sci. 70 (1978) 186.
[41] K.A. Dean, P. von Allmen, B.R. Chalamala, J. Vac. Sci. Technol. B 17 (1999) 1959.
[42] K. Hata, A. Takakura, Y. Saito, Ultramicroscopy 95 (2003) 107.
[43] T. Yamashita, K. Asaka, H. Nakahara, Y. Saito, Presented at the 7th Int. Vacuum Electron Sources Conf. (IVESC 2008), Queen Mary, University of London, London, August 4–6, 2008.
[44] A. Wadhawan, R.E. Stallcup II, K.F. Stephens II, J.M. Perez, I.A. Akwani, Appl. Phys. Lett. 79 (2001) 1867.
[45] N. Park, S. Han, J. Ihm, Phys. Rev. B 64 (2001) 125401.
[46] Z. Li, C.-Y. Wang, Chem. Phys. 330 (2006) 417.
[47] L.M. Sheng, P. Liu, Y.M. Liu, L. Qian, Y.S. Huang, L. Liu, S.S. Fan, J. Vac. Sci. Technol. A 21 (2003) 1202.
[48] Y. Saito, T. Matsukawa, T. Yamashita, K. Asaka, H. Nakahara, S. Uemura, Presented at the 14th Int. Display Workshops (IDW'07), Sapporo Convention Center Sapporo Japan, December 5–7, 2007.
[49] K. Kimoto, I. Nishida, Jpn. J. Appl. Phys. 16 (1977) 941.
[50] H.-P. Cheng, R.S. Berry, R.L. Whetten, Phys. Rev. B 43 (1991) 10647.
[51] E.W. Müller, Z. Naturforsh. 5a (1950) 473.